Observation and Differentiation of Unique High-Q Optical Resonances Near Zero Wave Vector in Macroscopic Photonic Crystal Slabs

Jeongwon Lee, Bo Zhen, Song-Liang Chua, Wenjun Qiu, John D. Joannopoulos, Marin Soljačić, and Ofer Shapira*

Research Laboratory of Electronics, Massachusetts Institute of Technology, 77 Massachusetts Avenue, Cambridge, Massachusetts 02139, USA

(Received 28 February 2012; published 8 August 2012)

We demonstrate and distinguish experimentally the existence of a special type of Fano resonances at $\mathbf{k} \approx \mathbf{0}$ in a macroscopic two-dimensional photonic crystal slab. We fabricate a square lattice array of holes in a silicon nitride layer and perform an angular resolved spectral analysis of the various Fano resonances. We elucidate their radiation behavior using temporal coupled-mode theory and symmetry considerations. The unique simplicity of this system whereby an ultralong lifetime delocalized electromagnetic field can exist above the surface and consequently easily interact with added matter, provides exciting new opportunities for the study of light and matter interaction.

DOI: 10.1103/PhysRevLett.109.067401 PACS numbers: 78.67.Pt, 42.79.Gn

The realization of high-quality factor cavities in photonic crystals has led in the past two decades to experimental observations of novel physical phenomena in both fundamental and applied research [1–12]. Modes supported by such cavities fall into two categories: (1) pure modes with infinite lifetimes that lie outside the light cone and (2) resonant modes with finite lifetimes that lie within the light cone and consequently can couple to radiation modes. A proposed surprising exception to the latter involves special Fano resonances of a macroscopic two-dimensional periodic photonic crystals slab, whose lifetimes are predicted to approach infinity as their crystal wave vector, $\mathbf{k}$, approaches zero within the light cone [13–15]. The only possibility for these special Fano resonances to completely decouple from the continuum of free-space modes is by mismatching their symmetries. It is the periodic nanostructure that determines the symmetry of the modes and the macroscopic large area that enables their approaching-to-infinity lifetime. In this Letter, we employ a centimeters square photonic crystal slab to demonstrate and distinguish $\mathbf{k} \approx \mathbf{0}$ nondegenerate Fano resonances with quality factors as high as 10^4 that extend over 10^8 unit cells. The photonic crystal, fabricated using interference lithography, consists of a square lattice array of holes in a Si_3N_4 layer with the periodicity of 320 nm. Through angle-resolved spectral measurements and temporal coupled-mode theory, we determined the resonances' quality factors and the various physical mechanisms that govern their value. Using symmetry considerations, we elucidate the behavior of the different resonances at $\mathbf{k} \approx \mathbf{0}$. The physical origin of Fano resonances in photonic crystal (PhC) slabs lies in the coupling between the guided modes supported by the slab and external plane waves, which occurs because of the periodic modulation of the dielectric constant. Typically all these Fano resonances have long lifetimes or high-quality factors (Q), but there is a special subset of them whose Q's have been proposed to approach infinity. In theory, in a perfect infinite periodic PhC slab, due to symmetry considerations, very unusual Fano "resonances" at $\mathbf{k} = \mathbf{0}$ have been predicted to completely decouple from the external world with an infinite radiative quality factor (Q_{rad}) despite lying within the light cone [13–15]. For $\mathbf{k}$ near zero, these unique guided resonances have an ultralong (but finite) lifetime, providing an efficient means to couple light in and out of the slab. In practice, due to the finite size of any experiment, the incoming and outgoing beams always include wave vectors with $\mathbf{k} > \mathbf{0}$, and hence the resonance lifetime is finite. Although this very unique behavior of Fano resonances in PhC slabs has been discussed theoretically [13–16], experimental verification of high-Q Fano resonances near $\mathbf{k} = \mathbf{0}$ over a macroscopically large area has yet to be demonstrated. The key challenge in observing these resonances is that in practical structures, in addition to limits imposed by material absorption, fabrication imperfections partially break the crystal symmetry which results in coupling of these Fano resonances to radiating modes. In addition, the mode itself needs to extend over a macroscopic area in order to support high Q_{rad}, posing a significant fabrication challenge.

Realizing high-quality factor resonances in photonic nanostructures requires both the careful consideration of the bulk material properties and the subwavelength structure geometry. Material absorption sets the upper bound of the attainable quality factor, while the structure geometry can be optimized to minimize scattering due to surface roughness and nonuniformities of the periodic structure. A favorable candidate for achieving high-quality factor resonances in the visible wavelength range light is a slab of Si_3N_4 deposited on top of a microns thick oxide layer of silicon wafer [17]. With a refractive index of 2.02, Si_3N_4 provides a sufficient index contrast with the SiO_2 below and air or fluids on top. We fabricated a large area square lattice PhC [18] with a periodicity of 320 nm and a unit cell consisting of a 55 nm deep, 160 nm in diameter cylindrical hole in a 250 nm thick Si_3N_4 layer (Fig. 1). Uniform periodic patterns were obtained on samples as large as 3 cm^2. We performed optical

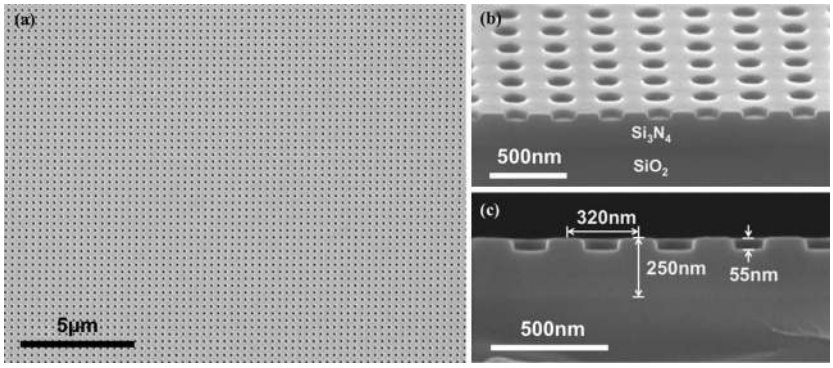

FIG. 1. SEM images of the fabricated PhC. (a) top view, (b) tilt view, and (c) side view SEM images of the fabricated PhC. The structure is made of a 250 nm thick Si_3N_4 with periodic cylindrical holes on top of a 6 μm thick SiO_2 layer with an average period of 320 nm, average hole diameter of 160 nm, and average hole depth of 55 nm.

characterization of the PhC slab using a supercontinuum laser source at small incident angles, θ, measured from the normal to the PhC plane towards the x axis [18]. The reflection spectra as a function of angle, for two orthogonal pump polarizations are presented in Figs. 2(a) and 2(d) revealing eight energy bands. To corroborate these results we used finite difference time domain simulation [19] to calculate the modes of the PhC [18]. Figures 2(c) and 2(f) show the dispersion curves of the eight lowest energy bands along the Γ-X line [$\mathbf{k}(\Gamma) = (0, 0)(2\pi/a)$, $\mathbf{k}(\mathbf{X}) = (0.5, 0)(2\pi/a)$, $\mathbf{k} = (k_x, k_y)$ and $\mathbf{k}_x = (\omega/c)\sin(\theta)$]. The four lower frequency bands are TE-like (numbered 1–4) and

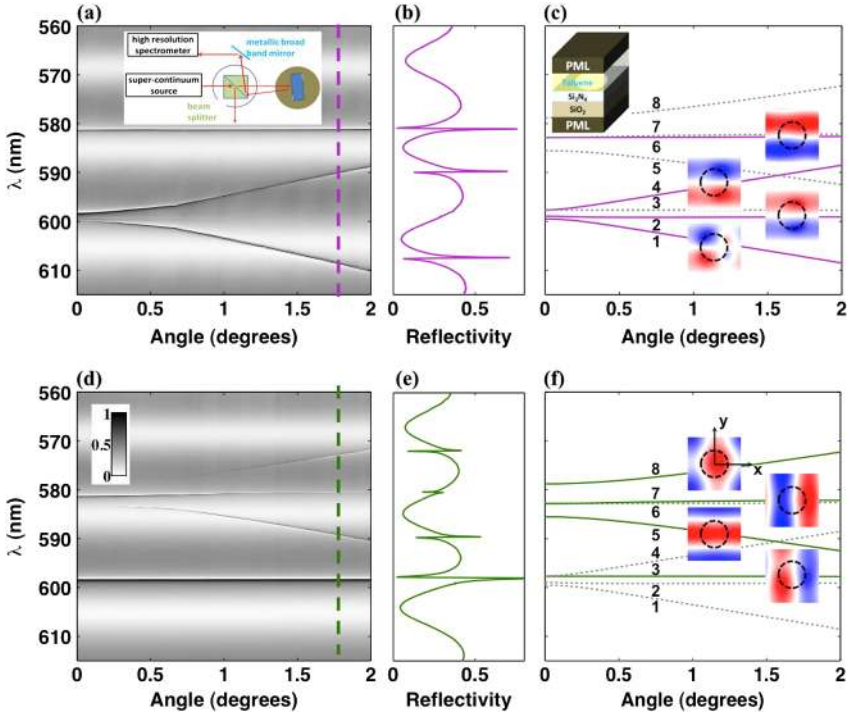

FIG. 2 (color online). Band diagrams of the PhC obtained from reflectivity measurement and finite difference time domain (FDTD) simulation. Reflectivity measurements of the PhC with (a) E_y and (d) E_x polarized beam. The inset shows a schematic of the experimental setup. (b),(e) A slice of the reflectivity spectrum at 1.8°. (c),(f) Band diagram of the eight lowest energy modes (measured at the Γ point) of the PhC obtained from FDTD simulation. The four lower frequencies modes (numbered 1–4) are TE-like and the four higher frequencies (numbered 5–8) are TM-like. Modes excited externally by an odd (even) polarized source with respect to the x axis are indicated as solid purple lines in (c) [solid green lines in (f)]; other modes are shown with gray dashed lines. Their E_z field profiles at the center of the Si_3N_4 layer at $\mathbf{k} = (0.01, 0)(2\pi/a)$ are also shown. The contour of the hole is shown with a black dashed circle. The inset depicts a schematic of the unit computational cell used in the numerical calculation. By applying periodic boundary conditions, the simulated structure becomes periodically infinite.

the four higher frequencies are TM-like (numbered 5–8). The presented E_z components of all eight modes are calculated at the center of the Si_3N_4 layer at $\mathbf{k} = (0.01, 0) \times (2\pi/a)$. The calculated resonant wavelengths are shifted by not more than $\pm 0.5\%$ from the measured spectra, well within the uncertainty of the measured periodicity or the value of the refractive index. An exception to that is the TE-like mode number 2 in Fig. 2(a) that appears to be very faint (almost missing): we explain the cause for this later.

It is evident from the measured spectral reflectivity of Figs. 2(a) and 2(d) that the incident beam may excite different modes of the PhC depending on its polarization. This can be understood from symmetry considerations: exciting the PhC slab with a source of one type of symmetry results in coupling to the modes of the same type of symmetry only. Note that moving away from Γ to X the symmetry group changes from C_{4v} to C_{1h} [20], reducing the number of irreducible representations from 5 to 2. The mirror reflection operation around the x axis leaves the modes of one irreducible representation unchanged, while the modes of the other irreducible representation are altered by a factor of -1. We can determine the symmetry of each mode by examining the mode profile of its E_z component as shown in Figs. 2(c) and 2(f). Modes 1, 2, 4, and 6 are altered by a factor of -1 under mirror reflection operation around the x axis and hence excited by E_y polarized source, while modes 3, 5, 7, and 8 are unchanged under the same operation and hence excited by E_x polarized source.

Figure 3 depicts the calculated $Q_{\mathrm{rad}}^{\mathrm{total}}$ of these eight bands. It reveals that while the doubly degenerate (at Γ) bands 3, 4, and 6, 7 have finite $Q_{\mathrm{rad}}^{\mathrm{total}}$ at $\mathbf{k} \approx \mathbf{0}$, the singly degenerate (at Γ) bands 1, 2, 5, and 8 have $Q_{\mathrm{rad}}^{\mathrm{total}}$ that go to infinity when approaching $\mathbf{k} = \mathbf{0}$. This can be qualitatively understood from symmetry arguments. As mentioned earlier, a mode at the Γ point belongs to one of five irreducible representations of the C_{4v} point group [15,20]. One of the

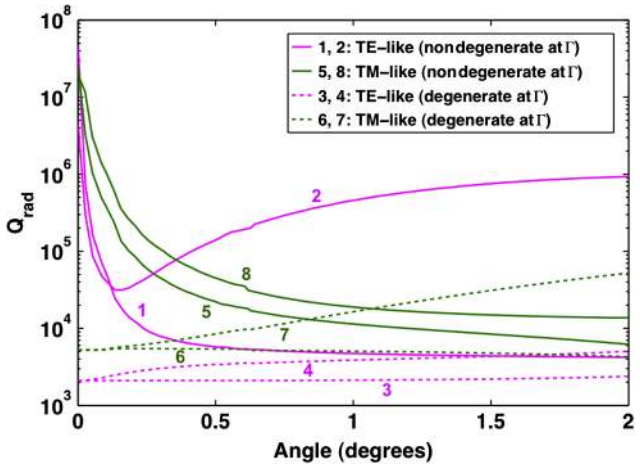

FIG. 3 (color online). Simulation results for radiative quality factors. The high-Q singly degenerate modes are shown with solid lines, while the doubly degenerate (at Γ) are shown with dotted lines.

irreducible representations is doubly degenerate and has the same symmetry as free-space modes, while the rest are all singly degenerate and are completely decoupled from free-space modes. As a result, $Q_{\mathrm{rad}}^{\mathrm{total}}$ of these four singly degenerate modes at the Γ point should be infinite despite lying within the light cone, while the doubly degenerate modes have finite $Q_{\mathrm{rad}}^{\mathrm{total}}$. As we move away from Γ to X the point group becomes C_{1h} and doubly degenerate modes split into two. The two irreducible representations of the C_{1h} point group share symmetry with the free-space modes and therefore $Q_{\mathrm{rad}}^{\mathrm{total}}$ become finite for all resonances, as is evident from the calculation.

To gain a deeper insight into the physics of the measured resonances, we developed a semianalytical temporal coupled-mode theory model [18] that accounts for the presence of guided leaky resonances in the Si_3N_4 layer [1,15]. We excited the model with an incident source propagating from the top and impinging onto the Si_3N_4 layer resonant cavity. From first-order perturbation to Maxwell's equation, energy conservation considerations, and neglecting second-order effects, we attained the following expression for the reflectivity of our sample:

$$|r_{\mathrm{PhC}}|^2 = \left| r_d - \frac{\gamma_{\mathrm{tol}}(\gamma_{\mathrm{tol}} r_d + \gamma_{\mathrm{SiO_2}} t_d)}{i(\omega - \omega_0) + \gamma_{\mathrm{tol}}^2/2 + \gamma_{\mathrm{SiO_2}}^2/2 + 1/\tau_{\mathrm{loss}}^{\mathrm{total}}} \right|^2, \tag{1}$$

r_d and t_d are the complex reflection and transmission coefficients of the sample without the square lattice of cylindrical air holes. γ_{tol} and γ_{SiO2} are the coupling strengths of the resonant mode to the top environment and the SiO_2 layer, respectively, and can be related to the quality factors by $\gamma_{\mathrm{SiO_2}}^2 = \omega_0/Q_{\mathrm{rad}}^{\mathrm{SiO_2}}$ and $\gamma_{\mathrm{tol}}^2 = \omega_0/Q_{\mathrm{rad}}^{\mathrm{tol}}$. From Eq. (1), it becomes obvious that there exist two temporal pathways: r_d, represents the direct transmission and reflection processes of the uniform stack, and the second term represents the guided resonances excited within the Si_3N_4 layers whose energy leaks into the far field. It is the superposition of the two physical processes that contributes to the typical narrow Fano line shapes superimposed on a Fabry-Perot-like background that are observed in the reflectivity spectra of Figs. 2(b) and 2(e). We fitted Eq. (1) to the measured spectra [18] and obtained the corresponding Q^{total}, defined as $1/Q^{\mathrm{total}} = 1/Q_{\mathrm{rad}}^{\mathrm{total}} + 1/Q_{\mathrm{loss}}^{\mathrm{total}}$, where $Q_{\mathrm{loss}}^{\mathrm{total}}$ includes losses from both material absorption and scattering due to fabrication imperfections. The results are summarized in Fig. 4, with an example of a fitted Fano resonance curve for the data measured at 0.8° of band 5. A complementary approach that also provides further intuitive understanding to calculate the reflection from such a structure was proposed by Pottage *et al.* [21].

Figure 4 reveals a clear distinction between the singly degenerate (modes 1, 2, 5, and 8) and the doubly degenerate (modes 3, 4, 6 and 7) modes at small angles. While the measured value of Q^{total} increases when approaching

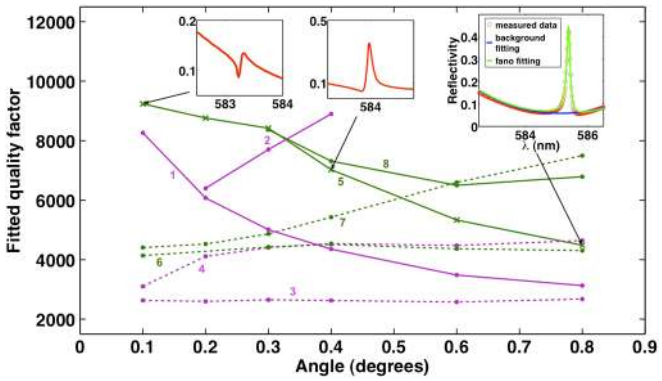

FIG. 4 (color online). Q^{total} values retrieved by fitting Eq. (1) to the measured data. Insets show the reflectivity spectra of the leaky mode 5 measured at three angles (0.1°, 0.4°, and 0.8°). The right inset depicts an example of the curve fitting process discussed in the text. Note the distinct higher quality factors of the singly degenerate modes close to the zero angle (i.e., zero wave vector).

$\mathbf{k} = \mathbf{0}$ for modes 1, 5, and 8, the doubly degenerate modes have decreasing or fixed values. We note that although Q^{total} as high as 10^4 are observed, the calculated $Q^{\text{total}}_{\text{rad}}$ (Fig. 3) of the singly degenerate modes are much greater at small angles, suggesting that close to $\mathbf{k} = \mathbf{0}$ the resonant energy decay is dominated by absorption and incoherent scattering from fabrication imperfections ($Q^{\text{total}} \approx Q^{\text{total}}_{\text{loss}} \approx 10^4$), both of which could be significantly reduced by improving the fabrication process. On the other hand, the four low-Q bands 3, 4 and 6, 7 in Fig. 4 have Q^{total} values that are comparable to the calculated $Q^{\text{total}}_{\text{rad}}$ and smaller than $Q^{\text{total}}_{\text{loss}}$. Indeed, FDTD calculations of the resonant mode show that the energy confinement is approximately unchanged within the plotted range of angles, suggesting that $Q^{\text{scat}}_{\text{loss}}$ is relatively constant in the considered range of angles. Apart from limiting the values of Q^{total} and hence the linewidth of the resonant line shapes, the presence of relatively large scattering loss and absorption compared to far-field radiation near normal incidence leads to reduced resonant amplitudes. Conversely, the decrease of $Q^{\text{total}}_{\text{rad}}$ away from normal provides a better match between $Q^{\text{scat}}_{\text{loss}}$ and $Q^{\text{total}}_{\text{rad}}$, which leads to an increase in the height of the features. This is consistent with Eq. (1), and also explains why band 2 appears only weakly in the measurement results shown in Fig. 2(a). Unlike other high $Q^{\text{total}}_{\text{rad}}$ modes whose values decrease rapidly away from the Γ point, the $Q^{\text{total}}_{\text{rad}}$ of the missing TE-like band 2 remains high (Fig. 3) for most angles, resulting in small reflectivity amplitudes which are harder to detect.

In conclusion, we experimentally differentiate and demonstrate the existence of a special class of resonances in PhCs with quality factors that could, in principle, approach infinity despite lying within the light cone. These nondegenerate Fano resonances are delocalized modes that decouple from the light cone states at $\mathbf{k} = \mathbf{0}$ due to symmetry considerations. A clear distinction between these modes and degenerate Fano resonances with finite Q^{total} at the Γ point is presented. With future improved fabrication that decreases the roughness and nonuniformities of the PhC slab, the current observed quality factors of $\sim 10^4$ can be significantly enhanced. The experimental realization of this mode has several important consequences: (1) the strongly enhanced field close to the PhC surface and the easy access to it provides a new platform for the study of light and matter interaction; (2) it offers an easy-to-fabricate structure that supports delocalized modes with ultrahigh quality factors; (3) it can be shown from coupled mode theory [22] that up to 50% of external radiation can be coupled to these strongly confined modes in symmetric PhC slabs, when one ensures that the Q-matching condition between the radiative lifetime, and the absorptive lifetime is satisfied; and (4) despite the macroscopically large area resonator, only a few high-Q modes are supported within a fairly broad frequency range. The delocalized nature of this mode is particularly important in applications where the interaction of an enhanced electric field with a macroscopic volume of matter can dramatically improve the performance of the process, such as in bimolecular sensing and organic light emitting devices. Furthermore, the realization of this novel resonance could enable the enhancement and the demonstration of new physical phenomena in laser physics, energy conversion, nonlinear optics, and optical filters.

B. Z., J. L., and M. S. were partially supported by S3TEC, an Energy Frontier Research Center funded by the U.S. DOE, Office of Science, and Office of Basic Energy Sciences, under Grant No. DE-SC0001299. B. Z. and M. S. were also partially supported by the U.S. Army Research Office through the Institute for Soldier Nanotechnologies under Contract No. W911NF-07-D0004. S.-L. C. and J. L. were also partially supported by the MRSEC Program of the NSF under Grant No. DMR-0819762. We thank Dr. Peter Bermel, Dr. Ling Lu, Dr. Ivan Celanovic, and Adrian Y. X. Yeng for fruitful discussions. J. L., B. Z., and S.-L. C. contributed equally to this work.

*To whom all correspondence should be addressed.
ofers@mit.edu

[1] J. D. Joannopoulos, S. G. Johnson, R. D. Meade, and J. N. Winn, *Photonic Crystals: Molding the Flow of Light* (Princeton University Press, Princeton, NJ, 2008).
[2] O. Painter, J. Vuckovic, and A. Scherer, J. Opt. Soc. Am. B **16**, 275 (1999).
[3] H. C. Y. Yamamoto and F. Tassone, *Semiconductor Cavity Quantum Electrodynamics* (Springer, New York, 2000), Vol. 169.
[4] R. K. Lee, Y. Xu, and A. Yariv, J. Opt. Soc. Am. B **17**, 1438 (2000).

[5] A. A. Erchak, D. J. Ripin, S. Fan, P. Rakich, J. D. Joannopoulos, E. P. Ippen, G. S. Petrich, and L. A. Kolodziejski, Appl. Phys. Lett. **78**, 563 (2001).
[6] S. Noda, M. Yokoyama, M. Imada, A. Chutinan, and M. Mochizuki, Science **293**, 1123 (2001).
[7] M. Fujita, S. Takahashi, Y. Tanaka, T. Asano, and S. Noda, Science **308**, 1296 (2005).
[8] A. Rosenberg, M. Carter, J. Casey, M. Kim, R. Holm, R. Henry, C. Eddy, V. Shamamian, K. Bussmann, S. Shi, and D. Prather, Opt. Express **13**, 6564 (2005).
[9] S. Noda, M. Fujita, and T. Asano, Nature Photon. **1**, 449 (2007).
[10] D. Englund, A. Faraon, I. Fushman, N. Stoltz, P. Petroff, and J. Vuckovic, Nature (London) **450**, 857 (2007).
[11] M. Ghebrebrhan, P. Bermel, Y. X. Yeng, I. Celanovic, M. Soljacic, and J. D. Joannopoulos, Phys. Rev. A **83**, 033810 (2011).
[12] S.-L. Chua, Y. Chong, A. D. Stone, M. Soljacic, and J. Bravo-Abad, Opt. Express **19**, 1539 (2011).
[13] P. Paddon and J. F. Young, Phys. Rev. B **61**, 2090 (2000).
[14] T. Ochiai and K. Sakoda, Phys. Rev. B **63**, 125107 (2001).
[15] S. Fan and J. D. Joannopoulos, Phys. Rev. B **65**, 235112 (2002).
[16] V. Pacradouni, W. J. Mandeville, A. R. Cowan, P. Paddon, J. F. Young, and S. R. Johnson, Phys. Rev. B **62**, 4204 (2000).
[17] E. S. Hosseini, S. Yegnanarayanan, M. Soltani, and A. Adibi, in *Frontiers in Optics* (Optical Society of America, Rochester, NY, 2008) p. FMG4.
[18] See Supplemental Material at http://link.aps.org/supplemental/10.1103/PhysRevLett.109.067401 for further details on the PhC fabrication, reflectivity measurement optical setup, FDTD computation, and coupled-mode theory.
[19] A. F. Oskooi, D. Roundy, M. Ibanescu, P. Bermel, J. D. Joannopoulos, and S. G. Johnson, Comput. Phys. Commun. **181**, 687 (2010).
[20] K. Sakoda, *Optical Properties of Photonic Crystals* (Springer, New York, 2001).
[21] J. M. Pottage, E. Silvestre, and P. S. J. Russell, J. Opt. Soc. Am. A **18**, 442 (2001).
[22] D. L. C. Chan, I. Celanovic, J. D. Joannopoulos, and M. Soljacic, Phys. Rev. A **74**, 064901 (2006).